Urban growth and spatial segregation increase disaster risk: Lessons learned from the 2023 disaster on the North Coast of São Paulo, Brazil

Cassiano Bastos Moroz[1], Annegret H. Thieken[1]

[1]Institute of Environmental Sciences and Geography, University of Potsdam, Potsdam, 14476, Germany

5   *Correspondence to*: Cassiano Bastos Moroz (bastosmoroz@uni-potsdam.de)

Abstract. Urban growth and the increase in urban poverty are important drivers of disaster risk. However, the influence of these processes on the dynamics of exposure and vulnerability remains uncertain. We hereby contribute to this discussion by presenting key lessons learned from the hazardous event that hit the North Coast of São Paulo (NCSP), Brazil, in February 2023. While the event was triggered by rainfall amounts of over 500 millimeters in a day, urban development processes also

10   influenced the disaster impacts. In this paper, we quantify these influences through a data integration approach combining empirical evidence on the historical evolution of urban settlements with damage mapping. We also evaluate the factors driving urban growth and spatial segregation in the region. We found out that the disaster impacts were largely attributed to historical urban growth, as 46% fewer buildings would have been damaged if the same event had happened around two decades earlier, i.e., in 2001. Also, precarious urban settlements were considerably more exposed and vulnerable to the event, as evidenced by

15   the density of damaged buildings, i.e., 12 times higher than in non-precarious settlements. We also observed strong patterns of spatial segregation in the NCSP. For instance, precarious settlements are much more frequent at hazardous locations, including on and at shorter distances from steep slopes. While this paper presents an analysis at the local level, the challenges of urbanization and growing intra-urban inequalities are global. Thus, these results reinforce the importance of accounting for such urban processes in disaster risk reduction interventions, and the urgent need for research efforts that go beyond the hazard

20   component, e.g., through an improvement of methods to simulate urban scenarios in the scope of disaster risk.

1 Introduction

The Sendai Framework 2015-2030 (UNISDR, 2015) highlights the need for understanding risk in all its dimensions of hazard, exposure, and vulnerability. However, exposure remains an under-researched component of the risk equation (Sieg & Thieken, 2022). The current IPCC report highlights that in the near term, changes in exposure and vulnerability will increase risks to

25   natural and human systems more than changes in hazard, driven by socioeconomic development, growing inequality, and urbanization (IPCC, 2022). These trends have already been observed over the last decades. Tellman et al. (2021) demonstrated that the proportion of the global population occupying areas exposed to large riverine floods has increased by 20% from 2000 to 2015. Similar findings of increasing global urban exposure to natural hazards were reported by Pesaresi et al. (2017). Thus, accounting for the dynamics of urban areas and their associated challenges (e.g., urban sprawl, poverty, and inequality) has

30 become essential in disaster risk reduction efforts. As highlighted by Portugali (2023), "the twenty-first century is to a large

extent the Age of Cities: cities have become the most dominant form of human settlement and way of life as more than half

the world's population live in cities". In fact, in 2018, 55.3% of the global population was urban. Half of them lived in small-

and medium-sized cities with less than 500,000 inhabitants (UN, 2018). Projections from the World Cities Report 2022 (UN-

Habitat, 2022) estimate that the global population living in cities is expected to increase further to 68% by 2050, with new

35 urban residents mostly concentrated in low- and middle-income countries (LMICs), including in Brazil where this study is set.

Urban exposure to disaster risk is even more expressive among the urban poor (IPCC, 2022). Worldwide, it is estimated that

around 1.6 billion people live in inadequate housing and 1 billion in informal settlements (UN-Habitat, 2022). In the Brazilian

context, as in other LMICs, urban inequalities and spatial segregation are often led by a complex system of competition

between the housing market and the "informal city" (Maricato, 2017). As a result, the urban poor are driven towards areas that

40 are less desirable to the market, frequently confined to hazardous locations such as floodplains and hillslopes (Maricato, 2017;

Ozturk et al., 2022; UN-Habitat, 2022). This has severe consequences on urban exposure. Ozturk et al. (2022) demonstrated

that informal settlements are between 20% to 500% more exposed to landslides as compared with formal urban areas when

evaluating the situation in five tropical cities across Africa and Asia. In another study conducted in the Kathmandu Valley, in

Nepal, Mesta, Cremen, and Galasso (2022) predicted significantly higher amounts of urban expansion towards hazardous

45 locations in urban neighborhoods of higher social vulnerability – often associated with lower socioeconomic status – when

compared with those of lower social vulnerability.

Apart from changing trends in exposure, the patterns of urban growth and spatial inequalities are also linked with changes in

hazard and vulnerability. Urban growth, especially the construction of irregular housing and settlements, can increase the

probability of hazard occurrence due to human modifications in the environment. These modifications impact slope stability

50 through processes such as vegetation deforesting, slope cutting, and inadequate drainage systems (Ozturk et al., 2022). They

can also alter the hydrological behavior of catchment areas with an increase in the proportion of impermeable surfaces (Pumo,

Arnone, Francipane, Caracciolo, & Noto, 2017). Vulnerability, both physical and social, is also influenced by the

socioeconomic status of the urban residents. Hallegatte et al. (2020) highlighted a few factors that make the urban poor more

vulnerable to hazards: a) a higher incidence of infectious diseases in the aftermath of events due to lack of drinking water

55 supply and sanitation, b) more physical damage to precarious buildings with low-quality materials that do not follow formal

construction standards, c) higher (relative) income losses during the event as for informal workers, and d) less governmental

support including protection measures and financial subsidies during the response and recovery phases.

A recent example of the large impacts of urban growth and inequalities on disaster risk is the event that hit the North Coast of

the São Paulo State (NCSP), in Southern Brazil, in February 2023. Rainfall amounts of over 500 millimeters in a day triggered

60 a multi-hazard event, displacing more than 2,000 residents and killing 65 people, mostly among the urban poor (Queiroz,

Lemos, Krunfli, Morimoto, & Araújo, 2023). The severe impacts of the disaster were not only attributed to the extreme rainfall

event. Fast urban expansion has been observed since the construction of the Rio-Santos highway, the main access to the region,

busted by investments in the tourism and energy industry sectors (CBH-LN, 2022; Daunt & Sanna Freire Silva, 2019;

Rosemback, Monteiro, Novaes Jr., Feitosa, & Ramos, 2010). The urban areas have been constrained by the mountainous topography of the region and the implementation of conservation policies (Rosemback et al., 2010), as roughly 80% of its territory is strictly protected according to the North Coast Ecological-Economic Zoning Plan (São Paulo State, 2017). The tourist attractivity of the region has also contributed to strong patterns of spatial inequalities and urban segregation by inflating the land value (Rosemback et al., 2010). In many locations, beachfront gated condominiums of second homes contrast with precarious settlements in environmentally fragile areas.

While the general picture of the disaster in the NCSP seems to be clear, we are unaware of any studies conducting quantitative analysis on the relationship between the extent of the disaster impacts and historical urban development in the region. In this context, the 2023 disaster provides an opportunity to understand how spatiotemporal patterns of urban growth, including urban segregation, have influenced the disaster impacts. We hereby present a few lessons learned from the event through a data integration approach combining empirical evidence on the historical evolution of urban areas with damage mapping. We also investigate the patterns and forces driving urban growth and segregation in the region. By doing so, we aim to support urban planning and disaster management practices through evidence-based analyses of the interplay between urban growth, segregation, and risk. We conduct this investigation by addressing the following research questions:

(1) To what extent did urban segregation influence (unequal) exposure to the disaster?

(2) How much of the disaster impacts could be attributed to changes in urban exposure?

(3) How have urban growth and segregation been manifested in the region over the last decades?

The paper is structured as follows. First, we introduce the case study area with a brief description of its environmental and socioeconomic characteristics. In the methodology and data section, we provide a detailed explanation of the key steps performed in the study: 1) the mapping of the physical damage to buildings during the event, 2) the attribution of this damage to changes in urban exposure and spatial segregation, and 3) the analysis of the historical patterns and drivers of urban growth and segregation. Then we present the main findings of our study for each research question, with further discussions. Finally, we draw some lessons learned in the concluding section.

2 Study area

The North Coast of São Paulo (NCSP) is an administrative sub-region of the State of São Paulo, in Southeast Brazil, and encompasses four municipalities: Caraguatatuba, Ilhabela, São Sebastião, and Ubatuba (São Paulo State, 2012). Together, these municipalities were home to 344,383 inhabitants in 2022, distributed within over 1.9 thousand square kilometers (IBGE, 2022). As a comparison, the population in the State of São Paulo was over 44 million in 2022 (IBGE, 2022). The NCSP is located along the mountain ranges of Serra do Mar and Serra da Bocaina (Daunt & Sanna Freire Silva, 2019), which contain some of the best-preserved fragments of the Brazilian Atlantic Forest (Ribeiro, Metzger, Martensen, Ponzoni, & Hirota, 2009). The geomorphology of the region is characterized by three main landforms: 15.8% of the area is formed by upland plateaus with elevations exceeding 1,000 meters; 12.7% by low-lying fluvial and coastal plains adjacent to the coastline; and the

remaining 71.5% by mountains and escarpments, which connect the previous landforms with elevations ranging from sea level up to 1,578 meters (ASF DAAC, 2015; IBGE, 2023). The prevalence of steep slopes, together with existing spatial planning policies and the implementation of several conservation areas on the Atlantic Forest, has constrained urban growth towards the few flatter areas along the coastline, where most of the public infrastructure is located (Rosemback et al., 2010). As a result,

100 over 81.6% of the land was covered by rainforest and sandbank vegetation, and only 3.9% by urban areas, as of 2022 (MapBiomas Project, 2022).

Despite the great level of conservation in the area, the NCSP has been pressured over the last decades with increasing demands for new urban areas. Information from the Brazilian census shows an increase of 195% in the population of the region from 1996 to 2022 (IBGE, 2022), which was accompanied by a fast expansion of urban areas (MapBiomas Project, 2022). The fast

105 population and urban growth have been driven by two main forces: high tourist attractivity, with increasing demands for housing (including second homes) and services; and improvements in road and industrial infrastructure for the oil and gas sectors, leading to increasing accessibility to the region (Daunt & Sanna Freire Silva, 2019; Daunt, Sanna Freire Silva, Bürgi, & Hersperger, 2021; Rosemback et al., 2010). While most of the urban settlements are located on flatter lands, newly urbanized areas have been expanding towards steeper slopes, on the transition zones between the coastal plains and the escarpments

110 (Daunt & Sanna Freire Silva, 2019; Daunt et al., 2021). The urban expansion towards hazardous locations such as steeper slopes has a strong impact on the exposure of urban settlements to disaster risk, as became evident with the disaster that hit the region in February 2023.

However, little is known about the patterns and drivers of urban dynamics in the NCSP, particularly in the context of disaster risk. The current study addresses this gap by investigating the interrelations between urban growth, segregation, and risk in the

115 context of the February 2023 disaster in the NSCP. After an initial evaluation of the event (Arango-Carmona et al., 2023), we decided to focus our analysis only on the region that was most impacted by the disaster. Therefore, we selected as a study area part of the municipality of São Sebastião, where most landslides and 64 out of the 65 fatalities occurred. This includes, from west to east, the coastal communities of Juquehy, Barra do Sahy, Baleia, Camburi, Camburizinho, and Boiçucanga, covering a total area of around 107 square kilometers. Figure 1 introduces the NCSP in the Brazilian context and further characterizes
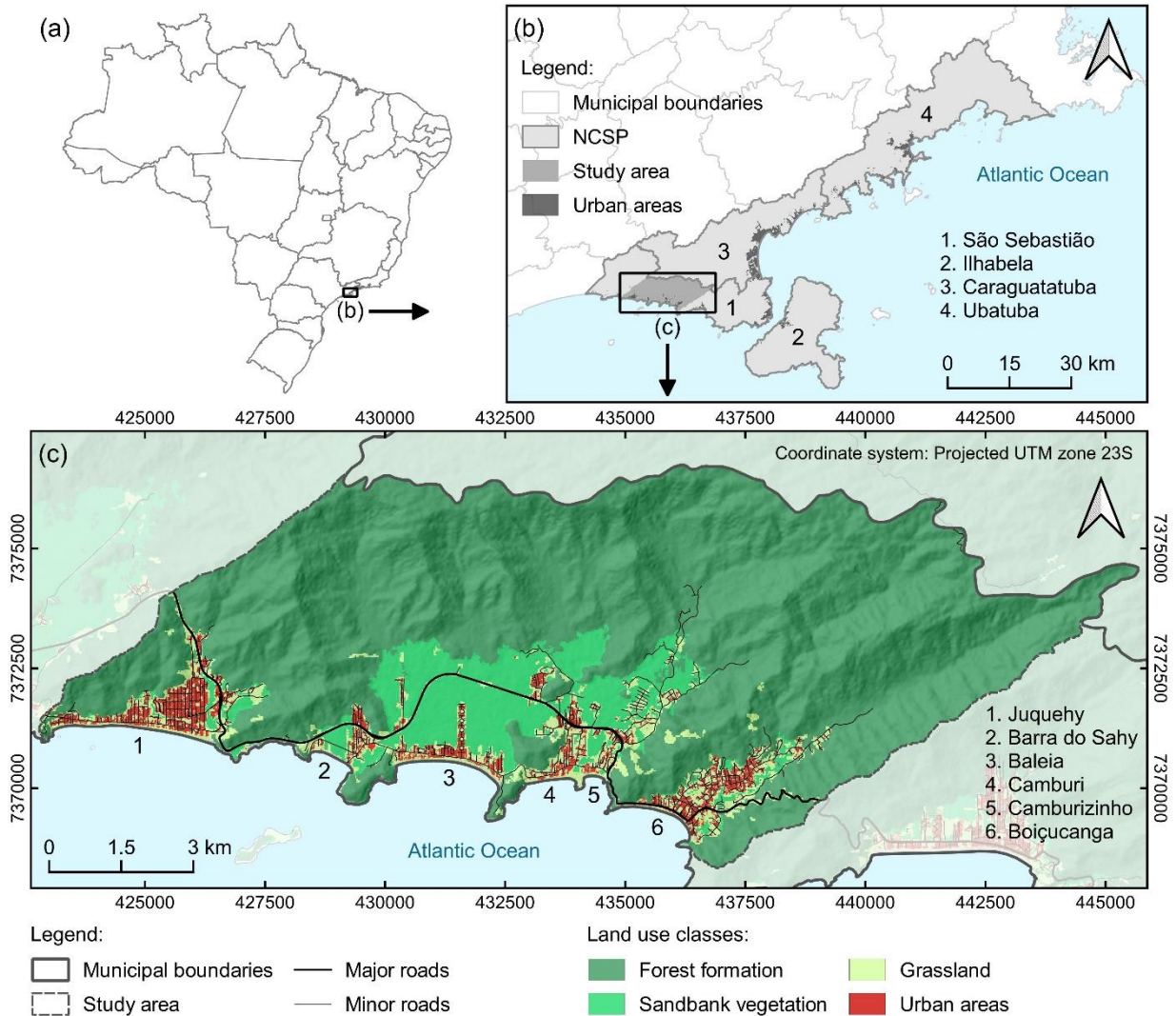
120 the study area.

Figure 1. Location map and characterization of the study area. (a) Location of the North Coast of São Paulo (NCSP) in Brazil; (b) Location of the study area in the NCSP; (c) Characterization of the study area. Data sources: ASF DAAC (2015), MapBiomas Project (2022), and © OpenStreetMap contributors (2023), distributed under the Open Data Commons Open Database License (ODbL) v1.0.

125

3 Methodology and data

Considering the availability and limitations of the data sources in the study area, we opted to structure our research methodology into two analyses. We first conducted an in-depth damage analysis to quantify and date the buildings damaged by the event, aiming to discuss the historical patterns of exposure and inequalities from the perspective of the 2023 disaster,

130   as described in sections 3.1 and 3.2. We later complemented this analysis by investigating the spatiotemporal patterns and drivers of urban growth and segregation in the region, as described in section 3.3.

3.1 Mapping the physical damage to buildings

For the initial analysis, we mapped and identified the physical damage to buildings through a visual interpretation of pre- and post-disaster aerial imagery at a spatial resolution of 0.1 meters. These images were obtained from DATAGEO, the
135   infrastructure of environmental geospatial data of the State of São Paulo (2023), and correspond to aerial photographs taken in 2022 (pre-disaster) and 2023 (post-disaster). As a preliminary step, we split the study area into a grid of regular cells, on which each cell could be visually interpreted at a scale of 1:1000 in QGIS software. We adopted these cells as a reference during the visual interpretation of the images to ensure the completeness of our mapping approach. For the visual interpretation, we mapped the individual damage to buildings as a point layer following the classification presented in Table 1. Both the
140   damage to buildings and the landslide or mudflow deposits were identified by comparing very high-resolution pre- and post-disaster images, as exemplified in Figure 2.

Table 1. Classification of physical damage to buildings.

Damage class	Description
Totally destroyed	(1) The building roof was visible in the pre-disaster but not in the post-disaster image, and (2) there were landslides and/or mudflow deposits at the (previous) location of the building in the post-disaster image.
Partially damaged	(1) The building roof was visible both in the pre-disaster and post-disaster images but with evidence of structural damage in the post-disaster image, and (2) there were landslides and/or mudflow deposits in the surroundings in the post-disaster image.

For reference, Figure 2 exemplifies the classification scheme presented in Table 1 with two cases representing one totally destroyed and one partially damaged building. The aerial images in the figure are the same adopted for the visual interpretation.
145   It is worth noting that we based our mapping approach solely on the visual interpretation of the roof structure, which is the most distinguishable building element in aerial imagery. Mapping other structural damage cannot easily be interpreted from aerial imagery and would require additional efforts not possible in this study. For example, an in-situ verification of the disaster impacts a few days after the event. Thus, our results do not represent any structural damage other than that to the building roof.
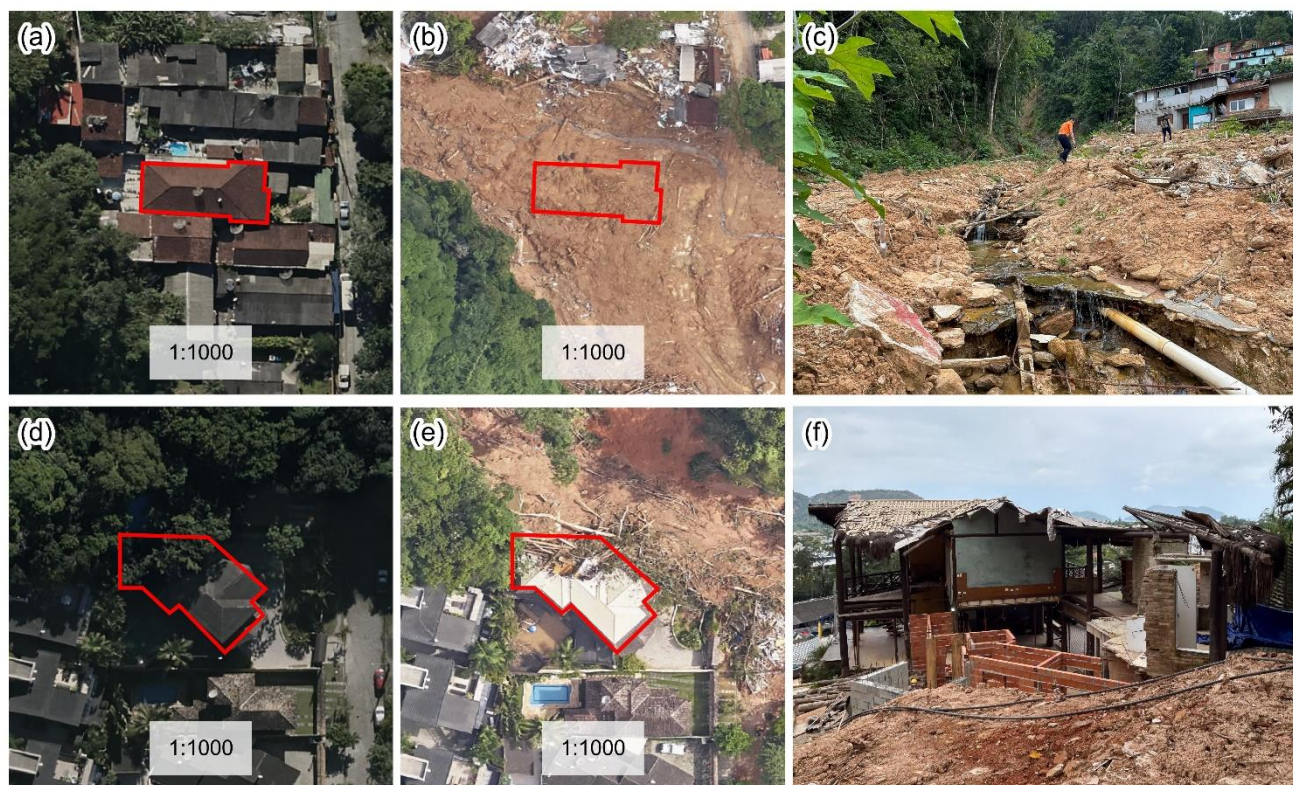
150 **Figure 2. Examples of total destruction and partial damage to buildings. (a) Pre-disaster aerial view of a building that was totally destroyed; (b) Post-disaster aerial view of the total destruction to the building (a); (c) Photograph from a field visit at the site where the building (a) was located, taken in November 2023; (d) Pre-disaster aerial view of a building that was partially damaged; (e) Post-disaster aerial view of the partial damage to the building (d); (f) Photograph from a field visit of the remnants of the building (d), taken in November 2023. Data source: Aerial imagery from DataGEO (2023).**

155 Having mapped the physical damage to buildings, we also integrated the spatial dimension of segregation into our analysis by classifying the mapped buildings according to the characteristics of the settlements where they are located. This classification was obtained through the intersection of the building points with the vector layer of *favelas* and urban communities (FUCs), as mapped by the Brazilian Institute of Geography and Statistics (IBGE, 2019). FUCs are the official denomination adopted by IBGE to refer to urban settlements that are predominantly formed by households without legal land rights and that fulfill at

160 least one of the following criteria: lack or precarity of public infrastructure; predominance of self-built infrastructure and/or houses; location at areas that are legally constrained by urban planning and/or environmental legislations (IBGE, 2024). For easier comprehension, we hereby differentiate FUCs from other urban settlements using the terms precarious and non-precarious urban settlements, respectively.

As a reference, Figure 3 exemplifies the morphological differences between a precarious and a non-precarious urban

165 settlement. The precarious settlement is constituted of smaller houses, mostly of fiber cement roofs, organized in irregular layouts, and connected via narrow and unpaved streets, thus indicating the lack or precarity of public infrastructure. In the case of the non-precarious settlement, houses are larger and covered by more resistant roof materials, mostly ceramic tiles. The

urban layout is more regular, and land parcels are separated by crisp boundaries. While these examples increase our understanding of some common morphological differences between both settlement classes, it is important to acknowledge

170   that urban areas are complex and heterogeneous. Thus, these figures only represent one case among many different configurations of precarious and non-precarious urban settlements.
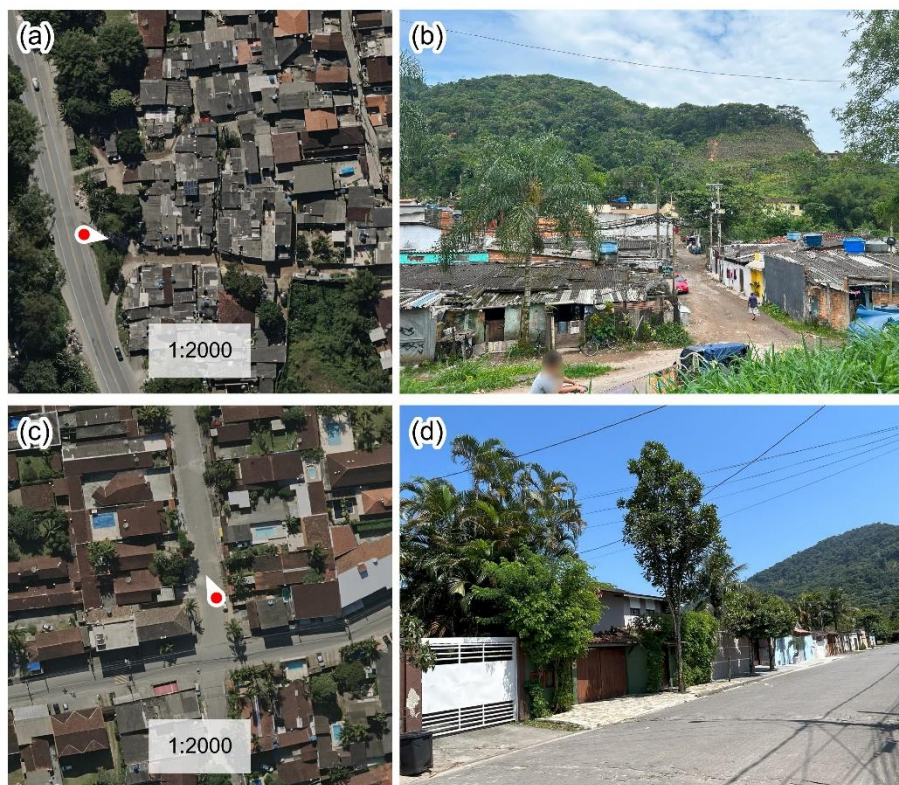
Figure 3. Morphological differences between a precarious and a non-precarious urban settlement. The arrows indicate the direction of the visual field in the photographs. (a) Aerial view of a precarious settlement; (b) Photograph from field visit at the location of (a), taken in November 2023; (c) Aerial view of a non-precarious settlement; (d) Photograph from field visit at the location of (c), taken in November 2023. Data source: Aerial imagery from DataGEO (2023).

It is important to outline that the adopted dataset of FUCs represents the situation in 2019. Thus, our analysis does not account for changes in urban classes at a particular location over time (i.e., from precarious to non-precarious or vice versa). Instead, it attributes newly urbanized cells to the urban class, either precarious or non-precarious, corresponding to the year 2019.

180   Despite this data limitation, this simplification seems reasonable in the specific context of the study area. An analysis of the historical imagery in Google Earth indicated that most urban morphologies (e.g., roof materials, size, and shape of buildings) have not changed over the last decades, thus providing evidence that the patterns of segregation also persisted.

3.2 Attributing damage to changes in urban exposure and spatial segregation

The mapping approach enabled us to understand the spatial distribution of the disaster impacts and the differences between
185   precarious and non-precarious urban settlements. However, the temporal dimension is also of great importance to evaluate to
which extent the disaster impacts could be attributed to historical changes in exposure. Hence, we addressed this question by
identifying the age of each building damaged by the event using very high-resolution aerial imagery. With these results, we
could evaluate, with high confidence, how much damage would have occurred if the same disaster event had happened decades
ago.
190   To identify the building age, we conducted the visual interpretation of a series of historical aerial imagery obtained from
DataGEO (2023), the infrastructure of environmental geospatial data of the State of São Paulo. The series of images includes
three sets representing the evolution of urban areas over three decades: two of them with a spatial resolution of 1 meter
corresponding to the years 2001 and 2010, and the remaining one with a finer spatial resolution of 0.1 meters corresponding
to the year of 2022, a few months before the event. While it was not possible to identify the exact year of construction, the
195   interpretation of these images enabled us to classify the buildings into three categories: buildings constructed a) before 2001,
b) between 2001 and 2010, and c) between 2010 and 2022. We finally adopted these classified buildings to investigate the
historical patterns of changes in exposure in the context of the 2023 disaster, also addressing the differences between precarious
and non-precarious urban settlements.

3.3 Understanding the patterns and drivers of urban growth and spatial segregation

200   So far, the previous analyses enabled us to understand the extent of the disaster impacts and its relationship with spatiotemporal
patterns of urban growth and segregation. However, little is known about the factors driving such urban development processes
in the region, and how these are associated with disaster exposure and vulnerability. In this study, we addressed this question
by conducting a statistical analysis to investigate the influence of several spatial factors on the historical development of urban
areas.
205   We started by mapping the historical footprint of urban growth and segregation in the study area based on two datasets. First,
we applied the World Settlement Footprint (WSF) Evolution layer to represent the spatiotemporal patterns of urban growth on
a yearly basis. The WSF Evolution layer is a 30-meter resolution global dataset outlining the yearly spatial footprint of urban
areas from 1985 to 2015. We then used the Brazilian national dataset of *favelas* and urban communities (FUCs) (IBGE, 2019)
to integrate the spatial dimension of segregation within the patterns of growth. We did it by intersecting the vector of FUCs
210   with the WSF maps.
Having mapped the historical footprint of urban development, we later evaluated its interrelations with several spatial factors,
thus aiming to identify the most important forces driving growth and segregation in the region. The objective was to understand
to which direction urban areas have expanded and how these patterns have changed over the years, and to identify potential
differences between precarious and non-precarious urban settlements.

215   To do so, we first classified the urban footprint maps into four categories representing the temporal evolution of growth: cells urbanized before 1985, from 1986 to 1995, from 1996 to 2005, and from 2006 to 2015. We then extracted the value distribution of each spatial factor within the boundaries of the urban areas for each temporal category independently. Using this temporal classification, we could investigate how urban growth manifested over the last decades concerning the analyzed spatial factors. During this step, we made a distinction between the distributions of precarious and non-precarious urban settlements so that

220   we could further elaborate on the patterns of segregation.

  To perform these analyses, we identified and selected a list of factors that could be relevant to explain the spatial trends of urban growth and segregation locally. We based our selection on the study of Allan, Soltani, Abdi, & Zarei (2022), who presented a systematic review of the key factors influencing land use and land cover changes in urban areas. The selection resulted in a final list of six factors, which are presented in Table 2 together with the data sources used.

225

Table 2. Adopted factors driving the spatial patterns of urban growth and segregation.

Factor	Data source(s)
Elevation	ALOS PALSAR RTC product (12.5 meters) (ASF DAAC, 2015)
Terrain slope	Derived from ALOS PALSAR RTC product (ASF DAAC, 2015)
Distance to slopes over 10 degrees*	Derived from ALOS PALSAR RTC product, based on Euclidean distance (ASF DAAC, 2015)
Distance to the main road	OpenStreetMap (OSM) layer, based on Euclidean distance (OpenStreetMap contributors, 2023)
Distance to rivers	Brazilian National Water Agency (ANA) layer, based on Euclidean distance (ANA, 2017)
Distance to the coastline	Visual interpretation of satellite imagery, based on Euclidean distance

*Minimum threshold to characterize a hillside as landslide-susceptible, as presented by Ozturk et al. (2022).

  The list of factors presented in Table 2 can be separated into two categories: topographical and contextual. The topographical factors include elevation, terrain slope, and distance to slopes over 10 degrees. These factors are important proxies of disaster exposure, given that topographical features such as slope steepness are often correlated with landslide susceptibility. In this

230   context, we also included the factor of distance to steep slopes (over 10 degrees) to account for the impacts of the landslide runout. The runout refers to the landslide debris that may travel downhill during the slope failure, reaching the areas surrounding the landslide initiation point. In its turn, the contextual factors include the distance to the main road, the distance to rivers, and the distance to the coastline. These factors represent the influence of infrastructure and natural features on the locational choice of urban areas, which might lead to patterns of urban segregation.

235   Finally, we also applied a Kolmogorov-Smirnov (KS) test to understand the influence of each factor on the patterns of segregation. The KS statistic is a metric that quantifies the (dis)similarity between two cumulative frequency distributions by calculating the maximum distance between them (Härdle, 2016). In our study, a great dissimilarity indicates that the analyzed factor has significant changes when comparing the distribution of precarious and non-precarious urban settlements. This provides evidence that such a factor has a major influence on the patterns of segregation. On the other hand, similar

240   distributions indicate that the factor is less relevant to explain differences in the location of both settlement classes.

4 Results and discussion

4.1 Absolute urban growth from 1985 to 2015

To provide an initial overview of the urban growth situation in the study area, we first quantified the absolute growth of precarious and non-precarious urban settlements at yearly intervals from 1985 to 2015. The results are presented in Figure 4.

245
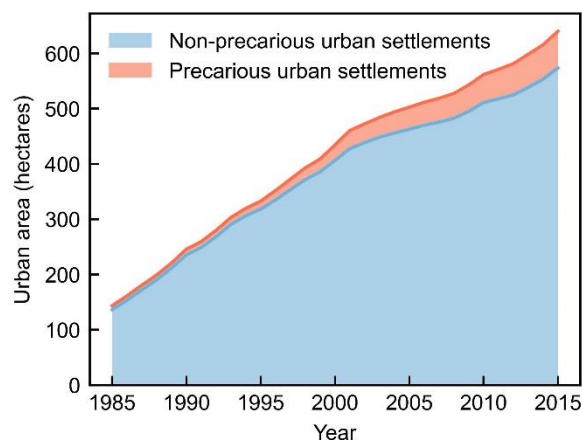
Figure 4. Yearly absolute growth of non-precarious and precarious urban settlements from 1985 to 2015. Data sources: DLR (2023) and IBGE (2019).

Figure 4 highlights an intense process of urban expansion in the study area. The total area of urban settlements increased 4.5

250 times from 1985 to 2015, i.e., from 143.5 to 640.0 hectares. Thus, the expansion of urban areas is a recent process, with most urban settlements built over the last three decades. As stated by Rosemback et al. (2010) and reinforced by Daunt et al. (2021), this fast expansion is largely attributed to the tourist attractivity and the increased accessibility to the region through the construction of the Rio-Santos highway in the late 1970s. This process was even more intensive when evaluating solely the expansion of precarious urban settlements. These settlements had an increase in the area of 9.2 times from 1985 to 2015, i.e.,

255 from 7.2 to 66.3 hectares. As a result, precarious urban settlements, which covered only 5.02% of all urban areas in 1985, doubled their spatial coverage to 10.36% in 2015. This evidences that urban poverty has increased in terms of spatial extent, with a considerable expansion of *favelas* and urban communities in the region.

4.2 Disaster impacts in the context of historical changes in (unequal) urban development

The quantification of urban growth evidenced an intense urbanization process in the region over the last decades, with a fast

260 expansion of precarious urban settlements. This evidences that the impacts of the 2023 disaster were likely influenced by urban development processes. To investigate this hypothesis, we first identified and mapped the buildings damaged by the event, classifying the building condition into partial damage and total destruction. We made a distinction between buildings in precarious and non-precarious urban settlements. Table 3 summarizes the results obtained from this analysis.

Table 3. Number of buildings damaged by the disaster, classified by damage class (partial damage or total destruction) and urban settlement class (precarious or non-precarious).

Urban settlement class	Damage class		Total
	Partial damage	Total destruction	
Non-precarious	29	13	42
Precarious	27	33	60
Total	56	46	102

According to our analysis, the 2023 event damaged 102 buildings in the study area, of which 56 were identified as partially damaged and 46 as totally destroyed. We also observed that 60 out of the 102 damaged buildings (~58%) were in precarious urban settlements. These results highlight the strong influence of segregation on disaster exposure in the region, given that precarious settlements covered only 10.36% of all urban extent in 2015 (DLR, 2023; IBGE, 2019), as presented in Figure 4. Thus, the density of buildings damaged by the disaster was over 12 times higher in precarious when compared with non-precarious settlements. These are in line with Ozturk et al. (2022), who demonstrated that informal settlements are between 20% to 500% more exposed to landslides when evaluating the situation in five tropical cities across Africa and Asia.

These patterns of segregation became even more evident when evaluating the damage severity. We observed that 27 out of the 56 buildings partially damaged by the disaster were in precarious urban settlements, which corresponds to around 48%. In the case of total destruction, 33 out of the 46 buildings were in precarious settlements, i.e., almost 72%. Thus, totally destructed buildings represented over 55% of all damages in precarious urban settlements, against only 31% in the case of non-precarious settlements. This evidences that precarious urban settlements were not only more exposed, but housing was also more physically vulnerable to the event.

For better visualization, Figure 5 illustrates the spatial distribution of the buildings damaged by the disaster, with a distinction between the damage class and the urban settlement class. The size of the circle indicates the frequency of buildings at each location. For reference, the total number of damaged buildings at each location is also presented in white next to the circles.

1. Juquehy | 2. Barra do Sahy | 3. Baleia | 4. Camburi | 5. Camburizinho | 6. Boiçucanga
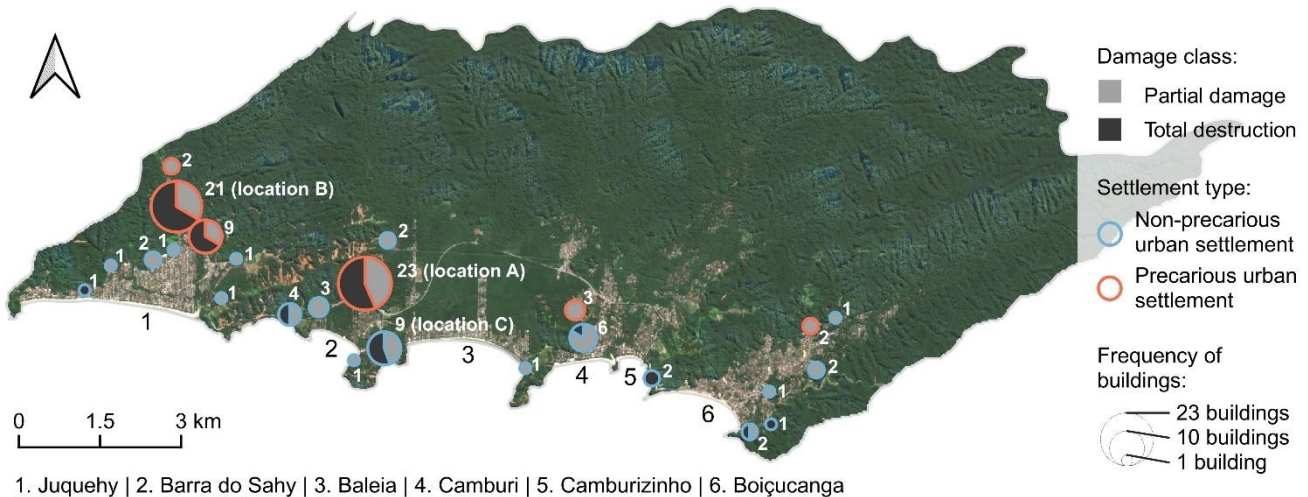
Figure 5. Spatial distribution of the physical damage to buildings, classified by damage class (partial damage or total destruction) and urban settlement class (precarious or non-precarious). The groups of buildings were determined through cluster analysis, wherein building points within a maximum distance of 300 meters were grouped. The highlighted locations (A, B, and C) are discussed in more detail in Figure 6 Figure 7. Data sources: Basemap from Image © 2023 Planet Labs PBC.

285

The extreme weather event that hit the NCSP in February 2023 triggered multiple landslides and mudflows across the region. As a result, buildings were damaged at multiple locations, largely concentrated at the borders of existing urban settlements, as illustrated in Figure 5. Regarding the patterns of segregation, we observed a few differences in the spatial distribution of the

290 damage when comparing both classes of urban settlements. Non-precarious settlements were hit by the disaster at several locations but often with a low amount of damage at each of them. Another characteristic of non-precarious settlements is the predominance of buildings with partial damage. In contrast, the situation in precarious urban settlements was characterized by more intense and severe damage. For instance, precarious settlements concentrated a considerably higher frequency of buildings damaged by the event, with a predominance of total destruction, as summarized in Table 3. An example can be

295 observed in the two most impacted communities, highlighted as locations A and B in Figure 5. Together, these communities encompassed 44 out of the 102 (~43%) buildings damaged by the event. Apart from the physical damage, Vila Sahy (location A in Figure 5) was also the region that concentrated most of the human losses (G1, 2023). To further elaborate on the causes leading to such large damage in these precarious communities, Figure 6 presents an in-depth evaluation of both locations.
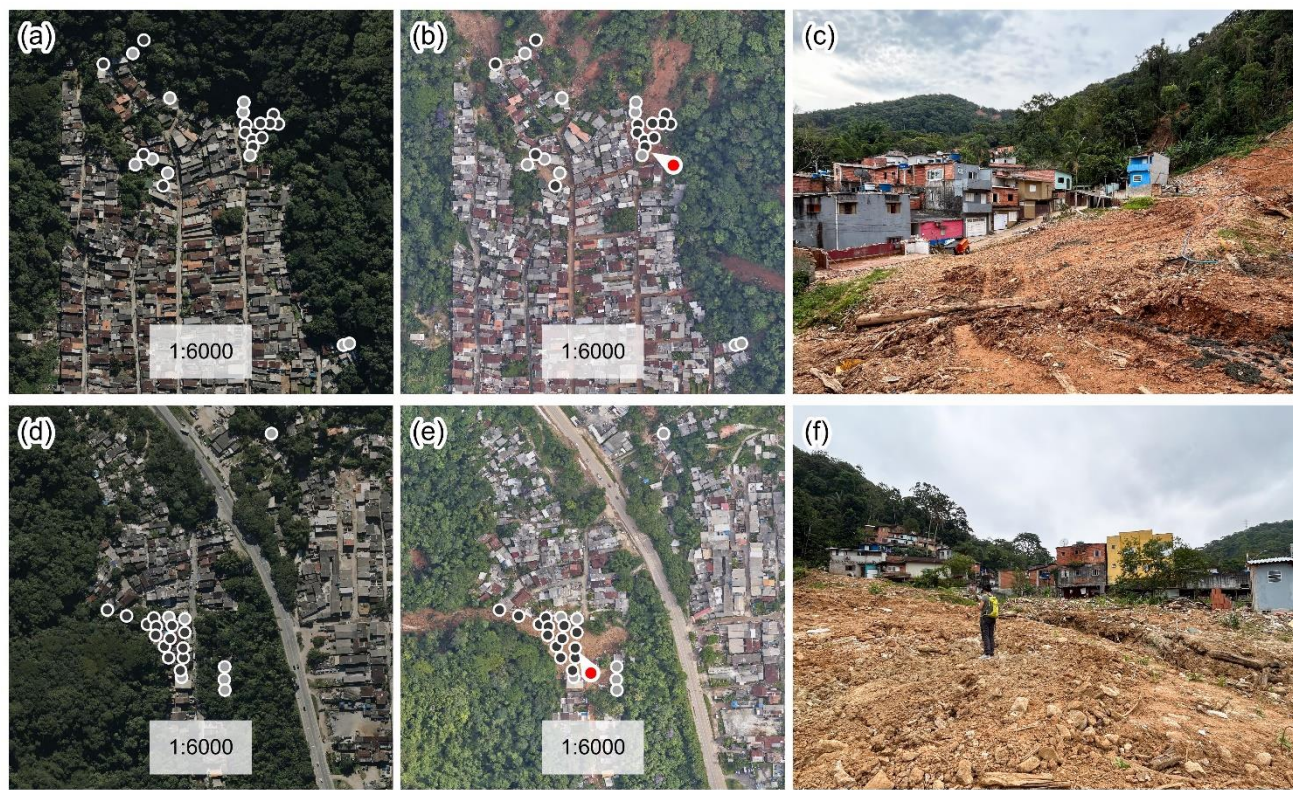
300 **Figure 6. Pre- and post-disaster damage analysis at the two most affected locations. The arrows indicate the direction of the visual field in the photographs. (a) Pre-disaster aerial view of a precarious urban settlement in Barra do Sahy (location A in Figure 5); (b) Post-disaster aerial view at the location of (a); (c) Photograph from field visit at the location of (a), taken in November 2023; (d) Pre-disaster aerial view of a precarious urban settlement in Juquehy (location B in Figure 5); (e) Post-disaster aerial view at the location of (d); (f) Photograph from field visit at the location of (d), taken in November 2023. Data source: Aerial imagery from**
305 **DataGEO (2023).**

In the case of the community in Barra do Sahy (Figure 6a to 6c), the severity of the damage was attributed to the overall impact of several landslides. As a result, 23 buildings were damaged in this region, of which 10 were classified as partially damaged and 13 as totally destroyed. The terrain topography also contributed to an intensification of the disaster impacts. The community occupies the lower elevations of a small catchment area, thus most of the surface flowing water is drained towards

310 the urban settlement. During the disaster, large amounts of mud and debris flows were channelized into the road network, as evidenced by the color of the street in the post-disaster image in Figure 6b. During our field visit in November 2023, we observed marks on building walls reaching almost 1 meter above the street level. A different situation was observed in the second most impacted community in Juquehy (Figure 6d to 6f). In this case, most of the damage was caused by the impacts of a single landslide over a densely populated urban area. This led to 21 damaged buildings, of which 7 were classified as partially

315 damaged and 14 as totally destroyed.

Despite the differences in the hazard processes, these locations share certain characteristics that are possibly associated with higher damage to buildings. First, they are characterized as precarious urban settlements, which are often more physically vulnerable to disasters such as floods and landslides, as discussed by Hallegatte et al. (2020). For instance, houses in precarious settlements are typically self-built, with poor-quality construction materials, and not following formal building standards. This

320 difference in vulnerability was evidenced by the considerably higher percentage of totally destroyed buildings in precarious settlements when compared with non-precarious settlements. The second shared characteristic is the large number of densely packed buildings, as observed in Figure 6a and 6d. As previously illustrated in Figure 3, precarious urban settlements are typically characterized by smaller houses and irregular land parcels, often leading to higher building densities when compared with non-precarious settlements. Thus, it is expected that localized hazardous processes such as landslides might cause greater

325 damage at these locations.

For comparative purposes, Figure 7 illustrates the most impacted non-precarious urban settlement: a neighborhood of high-income households located between the beaches of Barra do Sahy and Baleia (location C in Figure 5). A total of 9 buildings were damaged at this location, of which 5 were classified as totally destroyed and 4 as partially damaged. We also selected this location to reinforce that, although more frequent in precarious urban settlements, the occupation of hazardous locations

330 such as steep slopes also occurs in non-precarious settlements. The urban area illustrated in Figure 7 is settled on a hilly terrain, with elevations ranging from sea level up to 150 meters and slopes of over 20 degrees. Similar to the conditions in the precarious settlement in Barra do Sahy (Figure 6a to 6c), this urban area was impacted by several landslides, causing damage all across the region (Figure 7a and 7b). However, the low building density and the high quality of the building materials contributed to decreasing the number of buildings destroyed by the event. For example, Figure 7c represents a house settled

335 on a steep slope in the region. The building walls are made of reinforced concrete, probably with equally strong foundations

to bear the heavy loads of the construction. The building was hit by a landslide during the event, as evidenced by the presence of debris and tree branches in the surroundings, but its structure remained intact.
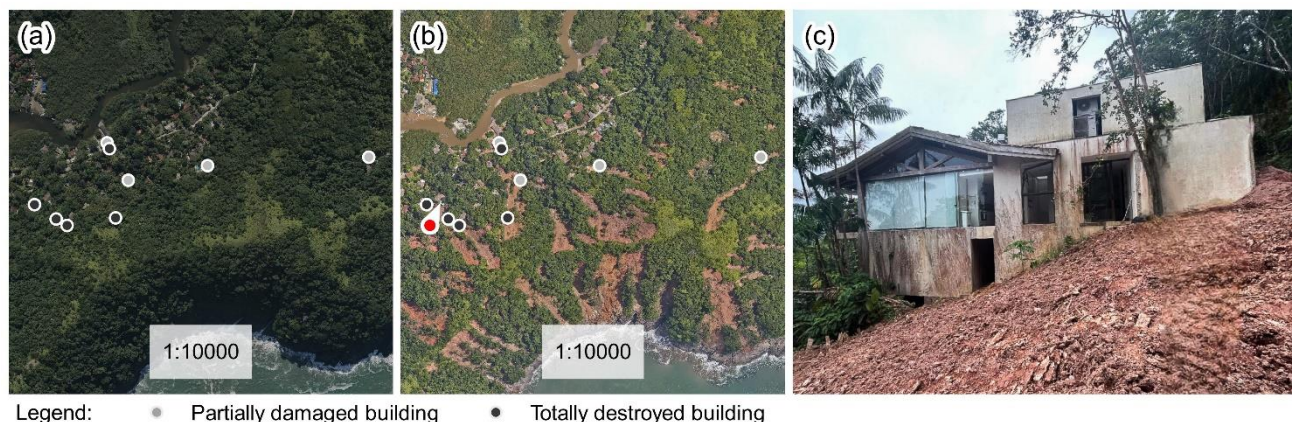
Figure 7. Pre- and post-disaster damage analysis. The arrows indicate the direction of the visual field in the photographs. (a) Pre-disaster aerial view of a non-precarious urban settlement between Barra do Sahy and Baleia (location C in Figure 5); (b) Post-disaster aerial view at the location of (a); (c) Photograph from field visit at the location of (a), taken in November 2023. Data source: Aerial imagery from DataGEO (2023).

As a second analysis, we evaluated to which extent the disaster impacts could be attributed to historical changes in urban exposure. We conducted this analysis by identifying the approximate age of each building damaged by the event having as a reference a set of high-resolution aerial images from 2001, 2010, and 2022. We also made a distinction according to the urban settlement class (precarious or non-precarious) and damage class (partial damage or total destruction). The results are presented in Table 4.

Table 4. Number of buildings damaged by the disaster, classified by urban settlement class (precarious or non-precarious), damage class (partial damage or total destruction), and period of construction (before 2001, 2002 to 2010, or 2011 to 2022).

Urban settlement class	Damage class (as of Feb. 2023)	Period of construction of buildings		
		Before 2001	2002 to 2010	2011 to 2022
Non-precarious	Partial damage	21	27	29
	Total destruction	8	12	13
Precarious	Partial damage	12	25	27
	Total destruction	14	28	33
All settlements and damage classes		55	92	102

The results indicate a considerable influence of historical changes in exposure on the impacts of the 2023 disaster. We observed that 33 out of 56 buildings (~59%) partially damaged by the disaster already existed in 2001. This difference was even more expressive when evaluating total destruction. Only 22 out of the 46 totally destroyed buildings (~48%) already existed in 2001. Thus, if the disaster event had happened in 2001, or a little more than two decades ago, it would have impacted only 55 out of the 102 buildings, or 46% fewer buildings when compared with 2023. These findings highlight the criticality of the urban development process on disaster risk in the NCSP. Moreover, they corroborate previous studies that reported historical changes

in global exposure to natural hazards (Pesaresi et al., 2017; Tellman et al., 2021). From 2000 to 2015, the increase in global population exposure was estimated at 20% for riverine floods (Tellman et al., 2021), 16% for tsunamis, and 21% for earthquakes (Pesaresi et al., 2017). Unfortunately, none of these studies have included landslides among the analyzed hazards. The results also highlight considerable differences in growth rates when evaluating the historical evolution of the number of buildings. We observed that 37 new buildings were constructed over 9 years from 2001 to 2010. In contrast, only 10 buildings were constructed over 12 years from 2010 to 2022. These figures point out the period from 2001 to 2010 as critical for the increase in the number of buildings exposed to the 2023 event. Unfortunately, we could not quantify the number of exposed buildings before 2001 because of the unavailability of high-resolution aerial imagery for comparison. However, it is important to mention that the analysis of urban growth patterns based on the WSF layer (see Figure 4) provides strong evidence that the disaster impacts would have been even lower if the event had happened decades before, i.e., in 1985. For instance, the statistics of urban growth point out the period from 1985 to 2001 as having the highest growth rate, of around 20.5 hectares per year. As a reference, the growth rate for the period from 2001 to 2010 was 12.0 hectares per year.

Another relevant finding is the distribution of buildings according to the urban settlement class. Precarious urban settlements concentrated 34 out of the 47 buildings that were recently constructed, i.e., after 2001. These settlements also presented higher relative growth rates. From 2001 to 2022, the number of buildings increased by 2.3 times in precarious and 1.4 times in non-precarious urban settlements. This faster expansion was previously discussed when evaluating the historical evolution of urban growth, as presented in Figure 4. However, the findings presented in Table 4 evidence that the expansion of precarious settlements has been accompanied by an increasing occupation of hazardous locations.

4.3 Patterns and drivers of urban growth and segregation

The analysis of the disaster impacts highlighted the influence of urban growth and spatial segregation on disaster risk, especially concerning the historical evolution of urban areas. In this section, we further elaborate on this topic by investigating the factors driving these urban development processes in the region.

Figure 8 illustrates the spatiotemporal patterns of urban growth and segregation in the study area, classified at decadal intervals between 1985 and 2015. An initial evaluation of the map evidences existing patterns of segregation when comparing the location of non-precarious and precarious urban settlements. Overall, we observed a high concentration of precarious settlements along the main road that provides access to the region, the Rio-Santos highway. Figure 8 also suggests that this highway seems to act as a physical barrier segregating both settlement classes. While non-precarious urban areas occupy the high-valued lands located in closer proximity to the coastline, most precarious settlements are located further away from the ocean, on the opposite side of the highway. Figure 8 also demonstrates the temporal evolution of growth in the study area, with considerable expansion since 1985. This is particularly evident in the expansion of precarious urban settlements. For example, most of the precarious urban community in Barra do Sahy – the red area located at number 2 on the map – was built after 1996. This recently urbanized area was also the most impacted by the 2023 disaster, as previously illustrated in Figure 6a to 6c.
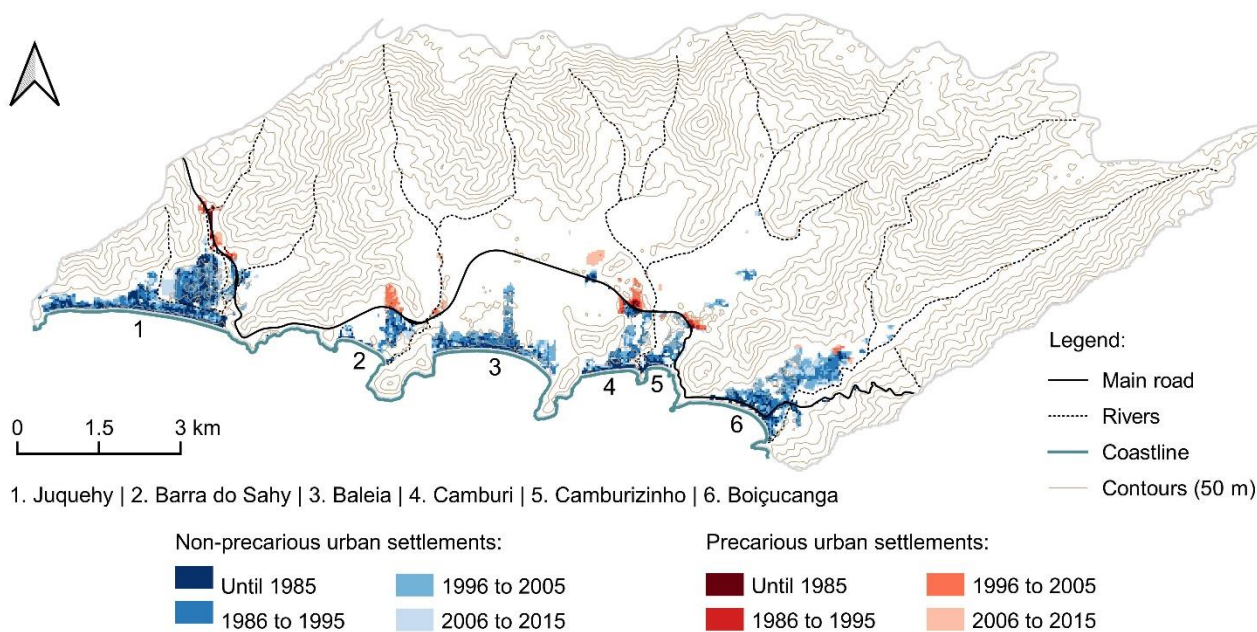
Figure 8. Spatiotemporal patterns of growth of non-precarious and precarious urban settlements from 1985 to 2015. Data sources: ANA (2017), ASF DAAC (2015), DLR (2023), IBGE (2019) and © OpenStreetMap contributors (2023), distributed under the Open Data Commons Open Database License (ODbL) v1.0.

To complement our analysis, Figure 9 further explores the spatiotemporal patterns of growth and segregation by quantifying the statistical distribution of the urban footprint as a function of the selected spatial factors, as presented in Table 2. We conducted the analysis independently for precarious and non-precarious urban settlements so that we could further elaborate on the segregation patterns. For reference, all spatial factors are represented in Figure 8.

The distributions of urban areas presented in Figure 9 highlight the existing patterns of segregation between non-precarious and precarious urban settlements. Regarding the topographical features, we observed that most urban areas, both non-precarious and precarious, are historically located at lower elevations (Figure 9a) and flatter terrains (Figure 9b). This can be observed by the high frequency of urban cells at elevations ranging from 0 to 10 meters, and terrain slopes ranging from 0 to 4 degrees. However, there is a crucial difference between both settlement classes. While non-precarious urban cells are almost entirely located within these low ranges, there is a non-negligible amount of precarious urban cells at elevations of up to 52 meters and slopes of up to 23 degrees starting after 1985. For instance, the frequency of urban cells at slopes steeper than 10 degrees is equivalent to 14% of all precarious urban settlements, against less than 3% in the case of non-precarious settlements (Figure 9b).
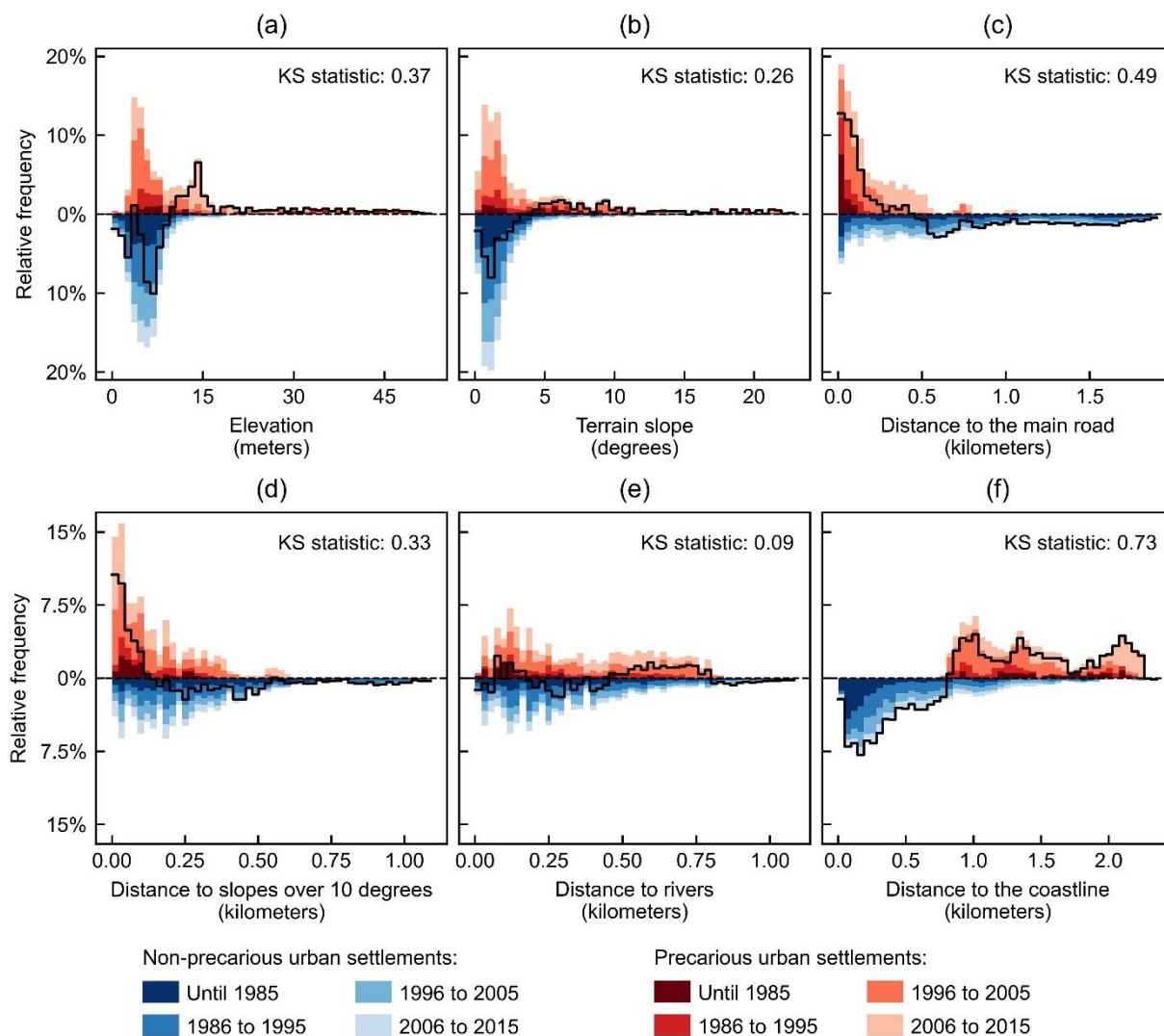
Figure 9. Frequency distribution of the spatial footprint of non-precarious and precarious urban settlements, discretized in timeframes, as a function of the factors: (a) elevation; (b) terrain slope; (c) distance to the main road; (e) distance to slopes over 10 degrees; (f) distance to rivers; (f) distance to the coastline. The continuous black line indicates the difference between the percentages of non-precarious and precarious urban settlements. See Table 2 for data sources.

Another manifestation of spatial segregation was observed when evaluating the distance to slopes steeper than 10 degrees (Figure 9d). Precarious urban settlements at shorter distances from steep slopes are much more frequent than non-precarious urban settlements. The share of urban cells at distances shorter than 100 meters from steep slopes represents 54.3% of all precarious urban settlements, in contrast to only 22.5% in the case of non-precarious settlements. This difference highlights the higher exposure of precarious urban settlements to landslide runouts, as became evident when evaluating the impacts of the 2023 disaster. Another important observation is that most of the urban areas at shorter distances from steep slopes were recently built, i.e., since 1996. Similar trends of urban development were also observed when evaluating the increasing

frequency of urban cells at higher elevations, i.e., since 2006 (Figure 9a). These findings corroborate the studies of Daunt &
420   Sanna Freire Silva (2019) and Daunt et al. (2021), who discussed a recent tendency of urban expansion toward higher
elevations and steeper slopes in the NCSP.

In addition to the frequency distributions, the results of the Kolmogorov-Smirnov (KS) test reinforce the relationship between
topographical factors and urban segregation. Elevation, distance to slopes steeper than 10 degrees, and terrain slope resulted
in a KS statistic of 0.37, 0.33, and 0.26, respectively. These values highlight existing dissimilarities between the distributions
425   of precarious and non-precarious urban settlements as a function of these factors. Thus, we can affirm that these topographical
factors are important variables to explain the patterns of spatial segregation between both settlement classes.

Apart from the topographical factors, contextual factors also proved to be of critical importance to understanding the patterns
of growth and segregation in the NCSP. Particularly, the distance to the coastline (Figure 9f) and the distance to the main road
(Figure 9c) proved to be key factors in orientating such patterns. However, we did not observe a clear pattern regarding the
430   influence of the distance to rivers, as reinforced by a low dissimilarity between the distributions, i.e., a KS statistic of 0.09
(Figure 9e). Thus, we will restrict our discussion to the previous two factors.

In the context of the distance to the coastline (Figure 9f), we observed a high concentration of precarious urban settlements at
locations that are more distant from the ocean, occupying lands that are less valuable to the tourism industry. This was
previously stated in the map presented in Figure 8. For instance, 99.6% of all precarious urban settlements are located at
435   distances greater than 800 meters from the coastline. The opposite situation is observed in the case of non-precarious
settlements. The frequency of urban cells located at distances shorter than 800 meters is equivalent to 73.5% of all non-
precarious urban settlements. The KS test also highlights the key influence of this contextual factor on the patterns of
segregation. The distance to the coastline presented the greatest dissimilarity among all analyzed factors, as demonstrated by
the KS statistic of 0.73. These figures highlight the importance of the distance to the coastline in orientating urban growth and
440   segregation in this touristic area. In addition, we also observed a recent trend of inland urban expansion for both settlement
classes, as demonstrated by the increasing concentration of urban cells at greater distances from the coastline from 1996
onwards. This trend is possibly explained by the scarcity of land available for construction, given the complex topography of
the region.

We also observed patterns of spatial segregation when evaluating the influence of the distance to the main road (Figure 9c).
445   The frequency of urban cells at distances shorter than 250 meters from the Rio-Santos highway is equivalent to 71.1% of all
precarious settlements, against only 25.4% in the case of non-precarious settlements. These differences in the location of both
settlement classes are also evidenced through the KS statistic of 0.49, the second highest among all analyzed factors. Two
potential explanations for this pattern are the lower land values along the highway and the facilitated accessibility to the road
system. For instance, certain areas of spontaneous growth including *favelas* and urban communities sometimes settle in closer
450   proximity to existing public infrastructure, including along roads or railways (Kuffer, Pfeffer, Sliuzas, Baud, & van
Maarseveen, 2017). However, it is important to highlight that this pattern has been slowly changing over the last decades, with
recently urbanized precarious settlements moving away from the highway, i.e., since 1996. In contrast, the distance to the main

road was demonstrated to be a factor of less importance in determining the location of non-precarious urban settlements. In this case, the frequency of urban cells is more constantly distributed across space, with the presence of urban areas at distances

455   of up to 2 kilometers from the highway.

The interrelations between the disaster impacts and the spatiotemporal patterns of urban growth and segregation pointed out key challenges associated with urban development processes in the NCSP. The increasing importance of the tourism industry since the construction of the Rio-Santos highway in the late 1970s contributed to a fast process of urban expansion, evidenced by the high quantity of second homes and services, e.g., hotels, restaurants, and others. This process has been accompanied by

460   a growing population of workers to fulfill the demands of this industry. However, the inflated land values along the coastline have limited the availability of affordable housing, thus orientating the expansion of lower-income neighborhoods towards low-valued areas. This was evident when evaluating the influence of the distance to the coastline on the location of precarious and non-precarious urban settlements. These challenges in the land market led to strong patterns of spatial segregation, with unequal exposure and vulnerability to hazards. For instance, this study demonstrated that precarious urban settlements are

465   considerably more frequent in hazardous locations, including on and at short distances from steep slopes. They were also the most impacted by the disaster, as evidenced by the large number of damaged buildings, most of which were totally destroyed.

5 Conclusion

In this study, we quantified the effects of urban development processes on the impacts of the 2023 disaster on the North Coast of São Paulo, in Southern Brazil. The analysis evidenced that the disaster impacts were highly influenced by a fast urban

470   expansion, of 450% from 1985 to 2015. Thus, if the same event had happened in 2001, it would have caused 46% less physical damage to buildings. Spatial segregation also played a role in the disaster impacts. Precarious urban settlements have expanded more rapidly than non-precarious settlements. The results also indicated that precarious settlements were more exposed and vulnerable to the hazard processes. The density of damaged buildings was around 12 times higher in precarious when compared with non-precarious settlements, with a predominance of totally destroyed buildings.

475   Several factors are associated with these unequal patterns of risk. First, precarious urban settlements are more frequent at hazardous locations, including on or at shorter distances from steep slopes, and this trend has increased over the last decades. This segregation pattern is possibly explained by the high land values driven by the tourist attractivity of the NCSP, as evidenced by the significant influence of the distance to the coastline on the location of these urban settlements. In addition, precarious urban settlements are often characterized by urban and housing conditions that exacerbate risk, e.g., higher building

480   densities and the prevalence of self-built houses with poor construction materials.

These findings demonstrate the challenges of urban expansion in a touristic and environmentally constrained area such as the NCSP, particularly in the context of urban poverty. The high tourist attractivity of the region leads to an expansion of urban areas and an increased need for a labor force to fulfill the demands of this industry. However, the inflated land values along the coastline limit the availability of affordable housing, thus orientating the expansion of urban settlements towards low-value

485 inland areas. Due to the mountainous topography of the region, these settlements end up getting confined between existing urban areas and the escarpments, often in hazardous locations.

Quantifying and acknowledging such spatial injustices in disaster exposure and vulnerability is essential to bring awareness to the challenges facing urban areas worldwide, especially regarding urban poverty. While this study presented the main lessons learned from a local event in Brazil, the challenges of urbanization and growing intra-urban inequalities are global. Thus, there

490 is an urgent need for more holistic research efforts that go beyond the hazard component, and for more sensitive and democratic approaches and interventions in disaster risk reduction.

Code/data availability

The data that support the findings of this study are openly available in: Bastos Moroz, Cassiano; Thieken, Annegret H. (2024), "Urban growth and spatial segregation increase disaster risk: Lessons learned from the 2023 disaster on the North Coast of

495 São Paulo, Brazil", Mendeley Data, V1, doi: 10.17632/2s44zm5433.1

Author contribution

C.B.M.: conceptualization, methodology, software, formal analysis, writing (original draft). A.H.T.: supervision, conceptualization, methodology, writing (review and editing).

Competing interests

500 None.

References

Allan, A., Soltani, A., Abdi, M. H., & Zarei, M. (2022). Driving Forces behind land use and land cover change: A systematic and bibliometric review. *Land*, *11*(8). https://doi.org/10.3390/land11081222

ANA. (2017). *Base hidrográfica ottocodificada multiescalas 2017 5k*. Retrieved from
505   https://metadados.snirh.gov.br/geonetwork/srv/api/records/f7b1fc91-f5bc-4d0d-9f4f-f4e5061e5d8f

Arango-Carmona, M. I., Moroz, C. B., Ferrer, J. V., Oberhagemann, L., Mohor, G. S., Skålevåg, A., … Thieken, A. H. (2023). A multi-hazard perspective on the São Sebastião-SP event in February 2023: What made it a disaster? *Proceedings of XXV Brazilian Symposium on Water Resources*, 1–9. Retrieved from https://anais.abrhidro.org.br/job.php?Job=14954

ASF   DAAC.   (2015).   *ALOS   PALSAR   Radiometric   Terrain   Corrected   (RTC)*.
510   https://doi.org/https://doi.org/10.5067/JBYK3J6HFSVF

CBH-LN. (2022). *Relatório de situação dos recursos hídricos do Litoral Norte*. Retrieved from https://cbhln.com.br/relatorio-de-situacao-dos-recursos-hidricos

DataGEO. (2023). DataGEO. Sistema Ambiental Paulista. Retrieved from https://datageo.ambiente.sp.gov.br/app/

Daunt, A. B. P., & Sanna Freire Silva, T. (2019). Beyond the park and city dichotomy: Land use and land cover change in the northern coast of São Paulo (Brazil). *Landscape and Urban Planning*, *189*(May), 352–361. https://doi.org/10.1016/j.landurbplan.2019.05.003

Daunt, A. B. P., Sanna Freire Silva, T., Bürgi, M., & Hersperger, A. M. (2021). Urban expansion and forest reserves: Drivers of change and persistence on the coast of São Paulo State (Brazil). *Land Use Policy*, *101*(May 2020), 105189. https://doi.org/10.1016/j.landusepol.2020.105189

DLR. (2023). *World Settlement Footprint (WSF) evolution (1985-2015)*. Retrieved from https://download.geoservice.dlr.de/WSF_EVO/

G1. (2023). Tragédia no litoral de SP: Mortes na Vila Sahy ocorreram no limite da área onde prefeitura permitiu ocupação. Retrieved October 3, 2023, from https://g1.globo.com/sp/sao-paulo/noticia/2023/02/24/tragedia-no-litoral-norte-de-sp-mapa-do-g1-mostra-o-rastro-de-destruicao-e-morte-na-vila-sahy-epicentro-do-desastre.ghtml

Hallegatte, S., Vogt-Schilb, A., Rozenberg, J., Bangalore, M., & Beaudet, C. (2020). From poverty to disaster and back: A review of the literature. *Economics of Disasters and Climate Change*, *4*(1), 223–247. https://doi.org/10.1007/s41885-020-00060-5

Härdle, W. K. (2016). *An introduction to statistics with Python*. Retrieved from http://www.springer.com/series/3022

IBGE. (2019). Favelas e comunidades urbanas. Retrieved October 1, 2023, from https://www.ibge.gov.br/geociencias/organizacao-do-territorio/tipologias-do-territorio/15788-favelas-e-comunidades-urbanas.html

IBGE. (2022). *IBGE cidades*. Retrieved from https://cidades.ibge.gov.br/

IBGE. (2023). *Cartas sobre a geomorfologia na escala 1:250,000*. Retrieved from https://www.ibge.gov.br/geociencias/informacoes-ambientais/geomorfologia/10870-geomorfologia.html?=&t=acesso-ao-produto

IBGE. (2024). *Sobre a mudança de aglomerados subnormais para favelas e comunidades urbanas*. Retrieved from https://biblioteca.ibge.gov.br/index.php/biblioteca-catalogo?view=detalhes&id=2102062

IPCC. (2022). *Climate change 2022: Impacts, adaptation and vulnerability*. Geneva, Switzerland.

Kuffer, M., Pfeffer, K., Sliuzas, R., Baud, I., & van Maarseveen, M. (2017). Capturing the diversity of deprived areas with image-based features: The case of Mumbai. *Remote Sensing*, *9*(4). https://doi.org/10.3390/rs9040384

MapBiomas Project. (2022). *Collection 8 of the annual land use land cover maps of Brazil*. Retrieved from https://brasil.mapbiomas.org/en/colecoes-mapbiomas/

Maricato, E. (2017). The future of global peripherical cities. *Latin American Perspectives*, *44*(2), 18–37. https://doi.org/10.1177/0094582X16685174

545   Mesta, C., Cremen, G., & Galasso, C. (2022). Urban growth modelling and social vulnerability assessment for a hazardous Kathmandu Valley. *Scientific Reports*, *12*(1), 1–16. https://doi.org/10.1038/s41598-022-09347-x

OpenStreetMap contributors. (2023). *Planet dump [Data file from 2023]*.

Ozturk, U., Bozzolan, E., Holcombe, E. A., Shukla, R., Pianosi, F., & Wagener, T. (2022). *How climate change and unplanned urban sprawl bring more landslides*. (August 2017).

550   Pesaresi, M., Ehrlich, D., Kemper, T., Siragusa, A., Florczyk, A., Freire, S., & Corbane, C. (2017). Atlas of the human planet 2017. Global exposure to natural hazards. In *Publications Office of the European Union*. https://doi.org/10.2760/19837

Portugali, J. (2023). Cities, complexity and beyond. In J. Portugali (Ed.), *Handbook on cities and complexity* (pp. 13–27). https://doi.org/https://doi.org/10.4337/9781789900125

Pumo, D., Arnone, E., Francipane, A., Caracciolo, D., & Noto, L. V. (2017). Potential implications of climate change and
555   urbanization on watershed hydrology. *Journal of Hydrology*, *554*, 80–99. https://doi.org/10.1016/j.jhydrol.2017.09.002

Queiroz, D., Lemos, L., Krunfli, M., Morimoto, T., & Araújo, Y. (2023). Impactos da tragédia no Litoral Norte de São Paulo deixam rastros sociais e ambientais. Retrieved January 16, 2024, from AUN USP website: https://aun.webhostusp.sti.usp.br/index.php/2023/07/18/impactos-da-tragedia-no-litoral-norte-de-sao-paulo-deixam-rastros-sociais-e-ambientais/

560   Ribeiro, M. C., Metzger, J. P., Martensen, A. C., Ponzoni, F. J., & Hirota, M. M. (2009). The Brazilian Atlantic Forest: How much is left, and how is the remaining forest distributed? Implications for conservation. *Biological Conservation*, *142*(6), 1141–1153. https://doi.org/10.1016/j.biocon.2009.02.021

Rosemback, R., Monteiro, A. M. V., Novaes Jr., R. A., Feitosa, F. da F., & Ramos, F. R. (2010). *Ampliando o olhar: Metodologia para estudo comparativo dos padrões de segregação socioespacial nas regiões de conurbação de São José
565   dos Campos e Jacareí , no Vale do Paraíba e Ubatuba , Caraguatatuba e São Sebastião, no Litoral Norte de SP*. (May), 1–11.

São Paulo State. (2012). *Lei complementar nº 1.166, de 09 de janeiro de 2012. Cria a região metropolitana do Vale do Paraíba e Litoral Norte, e dá providências correlatas*. Retrieved from https://www.al.sp.gov.br/repositorio/legislacao/lei.complementar/2012/lei.complementar-1166-09.01.2012.html

570   São Paulo State. (2017). *Decreto nº 62.913, de 08 de novembro de 2017. Dispõe sobre o Zoneamento Ecológico-Econômico*

do Setor do Litoral Norte, e dá providências correlatas. Retrieved from https://www.al.sp.gov.br/repositorio/legislacao/decreto/2017/decreto-62913-08.11.2017.html

Sieg, T., & Thieken, A. H. (2022). Improving flood impact estimations. *Environmental Research Letters*, *17*(6). https://doi.org/10.1088/1748-9326/ac6d6c

575 Tellman, B., Sullivan, J. A., Kuhn, C., Kettner, A. J., Doyle, C. S., Brakenridge, G. R., … Slayback, D. A. (2021). Satellite observations indicate increasing proportion of population exposed to floods. *Nature Portfolio Journal*, 1–30.

UN-Habitat. (2022). *World cities report 2022: Envisaging the future of cities*. Nairobi, Kenya.

UN. (2018). The world's cities in 2018. In *World Urbanization Prospects: The 2018 Revision*. Retrieved from https://www.un.org/en/development/desa/population/publications/pdf/urbanization/the_worlds_cities_in_2018_data_b
580 ooklet.pdf

UNISDR. (2015). *Sendai framework for disaster risk reduction 2015-2030*. Geneva, Switzerland.